

Effect of Void Network on CMB Anisotropy

Nobuyuki Sakai^{1*}, Naoshi Sugiyama², and Jun'ichi Yokoyama¹

¹Yukawa Institute for Theoretical Physics, Kyoto University, Kyoto 606-8502, Japan

²Department of Physics, Kyoto University, Kyoto 606-8502, Japan

ABSTRACT

We study the effect of a void network on the CMB anisotropy in the Einstein-de Sitter background using Thompson & Vishniac's model. We estimate both the Rees-Sciama effect and the gravitational lensing effect. As well as the Sachs-Wolfe effect, the Rees-Sciama effect can be appreciable even for multipoles $l \lesssim 1000$ of the anisotropy spectrum, if primordial voids exist at recombination, which is realized in some inflationary models associated with a first-order phase transition. The gravitational lensing effect, on the other hand, slightly smoothes the primary anisotropy; quantitatively, our results for the void model are similar to the previous results for a CDM model. Both effects, together, would give some constraints on the configuration or origin of voids with high-resolution data of the CMB anisotropy up to $l \sim 1000$. Those effects, on the other hand, are negligible for $l \lesssim 500$, which does not obstruct the determination of the cosmological model from the anisotropy spectrum.

Subject headings: cosmic microwave background, large scale structure

1. Introduction

The anisotropy of the cosmic microwave background (CMB) is an important probe of primordial fluctuations at recombination, which carries information on the cosmological parameters as well as the nature of dark matter (see, e.g., Hu, Sugiyama & Silk 1997). CMB photons, however, are also affected gravitationally by nonlinear structures between recombination and the present epoch. In fact, a network of voids filling the entire universe has been suggested by redshift surveys such as the CfA2 (Geller & Huchra 1989) and the SSRS2 (da Costa et al. 1994). Moreover, using such redshift surveys, El-Ad, Piran & da Costa 1996 (1996, 1997) and El-Ad & Piran (1997) quantified voids in the galaxy distribution and confirmed the description of a void-filled universe: they showed that $\sim 50\%$ of the volume is filled with the voids and that the

*E-mail: sakai@yukawa.kyoto-u.ac.jp

voids have a diameter of at least $40h^{-1}\text{Mpc}$ with an average underdensity of -0.9 . In this paper we investigate the effect of the void network on the CMB anisotropy in the Einstein-de Sitter background.

Rees and Sciama (1968, hereafter RS) showed that an evolving nonlinear structure perturbs the redshift of a photon passing through it by use of the “Swiss-cheese” model of overdensity. Later Thompson & Vishniac (1987, hereafter TV) estimated this RS effect in a void network model. First, they considered a spherical void in the Einstein-de Sitter background and derived an analytic expression of the redshift deviation $\delta T/T$ under the thin-shell approximation. Then, using this expression of $\delta T/T$, they calculated the variance of $\delta T/T$ for a universe filled with voids. As we will review in §2, the CMB anisotropy produced by the void network is of the order 10^{-6} if the present diameter of all voids is $60h^{-1}\text{Mpc}$ and if they have formed at $z < 10$; if the formation time is earlier, the anisotropy becomes larger. These results were supported by several authors (Sato 1985; Martínez-González, Sanz & Silk 1990; Martínez-González & Sanz 1990; Mészáros 1994; Mészáros & Molnár 1996; Panek 1992; Arnau, Fullana & Monreal 1993; Fullana, Arnau & Saez 1996; Shi, Widrow & Dursi 1996). Although density perturbations are usually assumed to be linear at the last-scattering surface (LSS), nonlinear voids can exist there if voids are originated by primordial bubbles which are nucleated in a phase transition during inflation (La 1991; Liddle & Wands 1991; Turner, Weinberg & Widrow 1992; Occhionero & Amendola 1994; Amendola et al. 1996; Baccigalupi, Amendola & Occhionero 1997; Baccigalupi 1997; Baccigalupi et al. 1997). Although the hypothesis of primordial voids is quite different from a conventional scenario, it may explain the present void-network structure and deserves further consideration. Therefore, more quantitative analysis of the RS effect for that case is important. One of the purposes of the present analysis is to calculate the power spectrum of the CMB anisotropy by extending TV’s analysis.

The lensing effect of density perturbations, on the other hand, has also been investigated by several authors (Blanchard & Schneider 1987; Kashlinsky 1988; Cole & Efstathiou 1989; Sasaki 1989; Tomita 1989; Tomita & Watanabe 1989; Fukushige, Makino & Ebisuzaki 1994; Linder 1990a, b; Cayón, Martínez-González & Sanz 1993a, b; Seljak 1996; Martínez-González, Sanz & Cayón 1997). It has been concluded, as a whole, that the effect is appreciable on arcminute angular scales for some models while it is negligible on degree scales. In particular, Seljak (1996) solved the shortcomings of the previous studies to include the nonlinear effects by modeling the power spectrum evolution in the nonlinear regime, and Martínez-González, Sanz & Cayón (1997) extended his method to study more general models; it was shown (Seljak 1996; Martínez-González, Sanz & Cayón 1997) that for a CDM model the lensing effect changes the CMB angular power spectrum C_l considerably for $l \gtrsim 1000$. This power spectrum approach can be applied to general models as long as the power spectrum of density perturbations is known. Because the power spectrum of a void-network universe is not obtained, however, we shall estimate the lensing effect in a different way. That is, we estimate the correction of the primary anisotropy, using TV’s formula of the scattering angle of a photon by a void. An advantage of our approach is that we make no approximation for nonlinearity nor relativistic effect.

In case nonlinear voids already exist at recombination — which is the case we are most interested in — we should also include the Sachs-Wolfe (1967, hereafter SW) effect of voids sitting on the LSS. Because that effect has already been investigated by Baccigalupi (1997) and Baccigalupi, Amendola & Occhionero (1997), we just make some comments on it in the last section.

The plan of this paper is as follows. In §2, we briefly review TV’s model and results, which we extend in the following sections. In §3, we calculate the temperature fluctuations caused by the RS effect of a void network. In §4, we investigate how the primordial fluctuations are modified by the gravitational lensing effect of a void network. §5 is devoted to summary and discussions.

2. Rees-Sciama Effect — Thompson & Vishniac’s Model and Results —

Because our analysis is based on TV’s model of a void-network universe and their analytical results, here we review them briefly. Consider a single spherical void in the Einstein-de Sitter background:

$$ds^2 = -dt^2 + a^2(t)(dr^2 + r^2d\theta^2 + r^2\sin^2\theta d\varphi^2) \quad \text{with} \quad a(t) = \left(\frac{t}{t_0}\right)^{\frac{2}{3}}, \quad (1)$$

where t_0 is the present time. The void itself is an empty spherical region, and hence a Minkowski spacetime:

$$ds^2 = -dt'^2 + dx'^2 + x'^2d\theta^2 + x'^2\sin^2\theta d\varphi^2, \quad (2)$$

where the prime denotes an internal coordinate. The matter surrounding a void is assumed to form a thin shell. From momentum conservation and energy conservation, respectively, Maeda & Sato (1983) and Bertschinger (1985) showed that the shell radius expands asymptotically as

$$r_v(t) \propto t^\beta \quad \text{with} \quad \beta \approx 0.13. \quad (3)$$

Figure 1 shows TV’s model of a photon passing through a spherical void. The subscripts 1 and 2 denote quantities at the time the photon enters the void and at the time it leaves, respectively. We define α as the angle formed between the direction of observation and the direction of the void’s center, $\delta\alpha$ as the scattering angle of a photon, d as the comoving distance of the void’s center, and d_{LSS} as the comoving distance of the LSS. The angles ψ_1 , ψ'_1 , ψ'_2 and ψ_2 are defined by reference to Figure 1.

TV applied double local Lorentz transformations at each void boundary. For example, the relation between the momentum vector just before entering a void, \mathbf{k}_1 , and the one just after passing the shell, \mathbf{k}'_1 , is expressed as

$$\mathbf{k}_1 \equiv E_1 \begin{pmatrix} 1 \\ \cos \psi_1 \\ \sin \psi_1 \\ 0 \end{pmatrix}, \quad (4)$$

$$\mathbf{k}'_1 \equiv E'_1 \begin{pmatrix} 1 \\ \cos \psi'_1 \\ \sin \psi'_1 \\ 0 \end{pmatrix} = E_1 \begin{pmatrix} \gamma_1 \gamma'_1 [1 + (v_1 - v'_1) \cos \psi_1 - v_1 v'_1] \\ \gamma_1 \gamma'_1 [\cos \psi_1 + (v_1 - v'_1) - v_1 v'_1 \cos \psi_1] \\ \sin \psi_1 \\ 0 \end{pmatrix}, \quad (5)$$

where velocities and Lorentz factors are defined as

$$v_1 \equiv a \frac{dr_v}{dt} \Big|_{t=t_1}, \quad v'_1 \equiv \frac{d(ar_v)}{dt'} \Big|_{t=t_1}, \quad \gamma_1 \equiv \frac{1}{\sqrt{1-v_1^2}}, \quad \gamma'_1 \equiv \frac{1}{\sqrt{1-v_1'^2}}. \quad (6)$$

In Appendix A we show the equations of the ‘‘Lorentz transformation’’ can be derived exactly from a general coordinate transformation in a curved spacetime.

After lengthy algebraic calculations, one obtains the redshift deviation and the scattering angle of a photon:

$$\frac{\delta T}{T} = (H_2 R_2)^3 \cos \psi_2 \left(3\beta - \frac{2}{3} \cos^2 \psi_2 \right) \equiv \Delta, \quad (7)$$

$$\delta \alpha \equiv -\psi_1 + \psi'_1 + \psi'_2 - \psi_2 = (H_2 R_2)^2 \sin(2\psi_2), \quad (8)$$

where H is the Hubble parameter, and $R \equiv ar_v$ is the proper length of the shell radius. The same results as equations (7) and (8) were also obtained by Martínez-González et al. (1990) in a different scheme using the ‘‘potential approximation’’.

Next, TV estimated the CMB anisotropy produced by a void network. Their model consists of randomly distributed, equally sized, and non-overlapped voids, which formed at some time t_f simultaneously. Divide the universe into shells of the comoving thickness $2r_v(t_0)$, as depicted in Figure 2. For each shell, the probability of a ray intersecting a void is given by

$$P = \frac{3}{2} F_0 \left(\frac{t}{t_0} \right)^{2\beta}, \quad (9)$$

where F_0 is the fractional volume of space occupied by voids and normalized at the present. The variance of $\delta T/T$ for each shell is

$$\sigma_{\text{RS,shell}}^2 \equiv \left\langle \left| \frac{\delta T}{T} \right|^2 \right\rangle_{\text{shell}} - \left\langle \frac{\delta T}{T} \right\rangle_{\text{shell}}^2, \quad (10)$$

where

$$\left\langle \left| \frac{\delta T}{T} \right|^2 \right\rangle_{\text{shell}} = P \int_0^{\frac{\pi}{2}} \Delta^2 \sin \psi_2 d\psi_2, \quad (11)$$

and Δ is given by equation (7). The net variance is

$$\sigma_{\text{RS}}^2 = \sum \sigma_{\text{RS,shell}}^2, \quad (12)$$

where the sum is over all the shells from t_f to t_0 . We can approximate it with an integral

$$\sigma_{\text{RS}}^2 = \int_{t_f}^{t_0} \sigma_{\text{RS,shell}}^2 \frac{dt}{\Delta t} \quad \text{with} \quad \Delta t \equiv 2a(t)r_v(t_0). \quad (13)$$

After an algebraic calculation, we obtain

$$\begin{aligned} \sigma_{\text{RS}} = & \frac{3}{2}(H_0 R_0)^{\frac{5}{2}} \left[\frac{3F_0}{5-24\beta} \left(\frac{2}{81} - \frac{8}{27}\beta + \beta^2 \right) \left\{ (1+z_f)^{\frac{5}{2}-12\beta} - 1 \right\} \right. \\ & \left. - \frac{4F_0^2}{5(1-6\beta)} \left(\beta - \frac{2}{15} \right)^2 \left\{ (1+z_f)^{\frac{5}{2}-15\beta} - 1 \right\} \right]^{\frac{1}{2}}. \end{aligned} \quad (14)$$

TV mentioned that the second term in equation (14), which stems from the second term in equation (10), goes to zero for $\beta = 2/15 \approx 0.133$. Although we choose $\beta = 0.13$ in this paper, $\langle \Delta \rangle \approx 0$ is still satisfied.

In this model there are three parameters: the radius of voids R_0 , the volume fraction F_0 , and the formation time z_f . Keeping in mind the results of El-Ad et al. (1996, 1997) and El-Ad & Piran (1997), we tentatively choose $R_0 = 40$ or $60h^{-1}\text{Mpc}$ and $F_0 = 2/3$ in the following. Figure 3 shows a plot of equation (14). We see that the net variance depends strongly on the formation time of voids. As TV concluded, the RS effect cannot make a dominant contribution to the CMB anisotropy if nonlinear voids form at $z < 10$; on the other hand, if voids form before or just after recombination as some inflationary models predicted, the RS effect may not be negligible.

3. Rees-Sciama Effect — Calculation of C_l —

As we discussed in the previous section, for the case where the primordial voids exist from recombination, more quantitative analysis of the RS effect is important. We extend TV's analysis and calculate the angular correlation function and its multipole moment, which are defined by

$$C(\theta) \equiv \left\langle \frac{\delta T}{T}(\boldsymbol{\theta}_A) \frac{\delta T}{T}(\boldsymbol{\theta}_B) \right\rangle_{\theta} \equiv \sum_l \frac{(2l+1)C_l}{4\pi} P_l(\cos \theta), \quad (15)$$

where $\boldsymbol{\theta}_A$ and $\boldsymbol{\theta}_B$ are angular positions with the separation angle θ . In general, in order to calculate the correlation function with density configuration in a real space, simulation-like computation is needed. However, if we evaluate

$$D(\theta) \equiv \left\langle \left[\frac{\delta T}{T}(\boldsymbol{\theta}_A) - \frac{\delta T}{T}(\boldsymbol{\theta}_B) \right]^2 \right\rangle_{\theta} = 2C(0) - 2C(\theta). \quad (16)$$

for each shell, we can sum up the contributions from all shells by using the same relation as equation (12).

Furthermore, for each shell, by the assumption of random distribution of voids and by the relation $\langle \Delta \rangle \approx 0$, the correlation function $C(\theta)$ for the case where two light rays A and B pass different voids becomes zero; this allows us to consider only one void in our calculation. Let us imagine a void projected on the celestial sphere, as depicted in Figure 4. The angles α_A , α_B , α_c , α_s , and ξ are defined by reference to Figure 4. We calculate $D(\theta)$ for each shell by

neglecting the curvature of the sphere in a local region around a void. Defining the midpoint of $\boldsymbol{\theta}_A$ and $\boldsymbol{\theta}_B$ as

$$\boldsymbol{\theta}_c \equiv \frac{\boldsymbol{\theta}_A + \boldsymbol{\theta}_B}{2} = (\alpha_c, 0), \quad (17)$$

the positions of $\boldsymbol{\theta}_A$ and $\boldsymbol{\theta}_B$ are written as

$$\boldsymbol{\theta}_A = \left(\alpha_c + \frac{\theta}{2} \cos \xi, \frac{\theta}{2} \sin \xi \right), \quad \boldsymbol{\theta}_B = \left(\alpha_c - \frac{\theta}{2} \cos \xi, -\frac{\theta}{2} \sin \xi \right). \quad (18)$$

Then we can calculate $D(\theta)$ for each shell with the expression

$$D(\theta)_{\text{shell}} = \frac{\alpha_m^2}{\alpha_s^2} P \frac{1}{\pi} \int_0^\pi d\xi \frac{2}{\alpha_m^2} \int_0^{\alpha_m} \alpha_c d\alpha_c [\Delta(\alpha_A) - \Delta(\alpha_B)]^2, \quad (19)$$

where the relation between ψ_2 and α (α_A or α_B) is

$$\sin \psi_2 = \frac{d}{r_2} \sin \alpha \quad \text{with} \quad d = 3t_0 \left[1 - \left(\frac{t}{t_0} \right)^{\frac{1}{3}} \right], \quad (20)$$

and the angular size α_s which corresponds to the void radius and the integral boundary α_m are defined as

$$\alpha_s \equiv \alpha|_{\psi_2=\frac{\pi}{2}} = \arcsin \left(\frac{r_2}{d} \right), \quad \alpha_m \equiv \alpha_s + \frac{\theta}{2}. \quad (21)$$

By numerical integration of equation (19), we obtain $D(\theta)$ for each shell. Then we sum up their values of all shells from t_f to t_0 . Figure 5 shows plots of $C(\theta)$ for $z_f = 5$ and for $z_f = 1000$. As we expected, the RS effect for $z_f = 5$ is negligibly small while it is not for $z_f = 1000$. Therefore, we plot the values of C_l only for the case of $z_f = 1000$. There is much difference in C_l between the cases of $R_0 = 40h^{-1}\text{Mpc}$ and of $R_0 = 60h^{-1}\text{Mpc}$. For the latter case the RS effect is large enough to be observed at the scale $l \approx 1000$ by the next Map and Planck experiments.

The dependence of the CMB fluctuations on the volume fraction of voids F_0 is easily understood: as equation (14) shows, $\delta T/T$ is proportional to $\sqrt{F_0}$, and C_l to F_0 , accordingly.

4. Gravitational Lensing Effect

We now turn to the lensing effect. First, we estimate the characteristic angular scale below which the lensing effect is appreciable, by calculating the angular excursion of a photon on the LSS, $\boldsymbol{\delta\theta}$. The lens equation for a single void in the thin lens approximation is

$$\boldsymbol{\delta\theta}_{\text{one void}} = W\delta\alpha\boldsymbol{l} \quad \text{with} \quad W \equiv \frac{d_{\text{LSS}} - d \cos \alpha}{d_{\text{LSS}}}, \quad (22)$$

where the vector $\boldsymbol{l} \equiv \boldsymbol{\delta\theta}/|\boldsymbol{\delta\theta}|$ has been introduced in Figure 1. In reality this thin lens equation can be derived exactly from null geodesic equations, as shown in Appendix B.

Replacing $\delta T/T$ with $W\delta\alpha$ in TV's calculation of σ_{RS} in §2, we find

$$\begin{aligned} \sqrt{\langle |\delta\boldsymbol{\theta}|^2 \rangle} &= (H_0 R_0)^{\frac{3}{2}} \frac{\sqrt{F_0}}{\sqrt{z_{\text{LSS}} + 1} - 1} \left[\frac{1}{3(6\beta - 1)} - \frac{\sqrt{z_{\text{LSS}} + 1}}{9\beta - 1} + \frac{z_{\text{LSS}} + 1}{18\beta - 1} \right. \\ &\left. - (z_f + 1)^{\frac{3}{2} - 9\beta} \left\{ \frac{1}{3(6\beta - 1)} - \sqrt{\frac{z_{\text{LSS}} + 1}{z_f + 1}} \frac{1}{9\beta - 1} + \frac{z_{\text{LSS}} + 1}{z_f + 1} \frac{1}{18\beta - 1} \right\} \right]^{\frac{1}{2}}. \end{aligned} \quad (23)$$

We draw a plot of equation (23) in Figure 7, assuming $z_{\text{LSS}} = 1000$. The lensing effect also depends on the formation time of voids, though the dependence is not so strong as in the case of the RS effect. The typical angular scale of lensing is several arcminutes.

These angles, however, are not directly observable; we would rather calculate the dispersion of the relative angular separation θ , which is defined as

$$\sigma_{\text{gl}}(\theta) \equiv \frac{1}{\sqrt{2}} \langle |\delta\boldsymbol{\theta}_A - \delta\boldsymbol{\theta}_B|^2 \rangle_{\theta}^{\frac{1}{2}}. \quad (24)$$

σ_{gl} is, like the case of the RS effect, proportional to $\sqrt{F_0}$. The values of $\sigma_{\text{gl}}(\theta)$ for each shell and their sum are computed just like the computation of $D(\theta)$ in §3. Figure 8 shows a plot of $[\sigma_{\text{gl}}(\theta)/\theta]_{\theta=0.01\text{arcmin}}$ for each shell. Voids at $z \approx 50$ make the largest contribution to the CMB anisotropy: due to the factor W in equation (22), no effect arises from voids on the LSS, contrary to the case of the RS effect. To show that the dependence on the formation time z_f is not so strong in this case, we calculate $\sigma_{\text{gl}}(\theta)$ for several values of z_f , and some examples are presented in Figure 9. We note that the results are similar to the previous results for a CDM model (Seljak 1996; Martínez-González, Sanz & Cayón 1997), though models and methods are quite different.

Once $\sigma_{\text{gl}}(\theta)$ is known, we can calculate the lensing effect on the CMB fluctuations. Here we adopt the approximate formula of Seljak (1996) for the lensed correlation function:

$$\tilde{C}(\theta) = \frac{1}{2\pi} \int_0^\infty l dl e^{-\sigma_{\text{gl}}^2(\theta)l^2/2} C_l J_0(l\theta). \quad (25)$$

An example of the CMB anisotropy spectrum including lensing is presented in Figure 10a. As Seljak (1996) and Martínez-González et al. (1997) showed for a CDM model, the lensing effect is to slightly smooth the main features appearing in the spectrum. To see the dependence on R_0 and z_f , we show the relative changes of the spectrum due to lensing for several cases in Figure 10(b), (c). In contrast with the case of the RS effect, the lensing effect has a weak dependence on the formation time.

5. Summary and Discussions

We have investigated the effect of the void network on the CMB anisotropy for TV's model, where many voids are distributed in the Einstein-de Sitter background. In particular, we have calculated the RS effect and the gravitational lensing effect separately.

As TV and other authors have already shown, the RS effect cannot make a dominant contribution to the CMB anisotropy in conventional scenarios like a CDM model, where nonlinear structure are formed at late time ($z_f < 10$). Hence, as to the RS effect, we have concentrated our attention on the case where primordial voids already exist at recombination, which is the case in some inflationary models. Calculating the angular power spectrum C_l , we have found that the RS effect can be appreciable in that case.

As we have mentioned in §1, however, the SW effect of voids lying on the LSS is also important and should be included. On the contrary, Baccigalupi, Amendola & Occhionero (1997) claimed that the RS effect is negligible with respect to the SW effect, showing that the RS effect results from a partial cancellation of the redshift occurring during the void crossing, namely the SW effect, with the blueshift occurring at either shell crossing. We agree that, if we estimate the redshift distortion by a single void, the SW effect is much larger than the RS effect. What we would like to remark is that the number of voids between the LSS and us, which contribute to the RS effect, is much larger than the number of voids lying on the LSS. Hence, the total distortion of the redshift of photons by the RS effect can also be appreciable. In this sense, together with the analysis of the lensing effect, our work is complementary to that of Baccigalupi, Amendola & Occhionero (1997) and Baccigalupi (1997) for the probe of inflationary models associated with a first-order phase transition.

As for gravitational lensing, the effect of nonlinear voids has not been investigated so far. Our present work is the first trial of that investigation without any approximation for nonlinearity nor relativistic effect. We have shown how the primary anisotropy is smoothed out for some values of the void radius R_0 and of the formation time z_f . We have found that our results are similar to those for a CDM model (Seljak 1996; Martínez-González, Sanz & Cayón 1997).

Our results as a whole suggest that, if the real universe is filled with nonlinear voids, they make some appreciable effects on the CMB anisotropy even for multipoles $l \lesssim 1000$. Those effects are expected to give some constraints on the configuration or origin of voids, particularly on the inflationary models in which primordial bubbles are nucleated, with the next generation of CMB satellites.

From another point of view, this multi-void model describes the extremely nonlinear universe that can be extrapolated from the distribution of luminous galaxies. Our results for $z_f = 1000$ provide the maximal contribution by nonlinear structure to the CMB anisotropy. We may, therefore, also conclude that, if one wants to determine the cosmological model from multipoles $l \lesssim 500$ of the anisotropy spectrum, the effect of nonlinear structure can be ignored.

Acknowledgments

We thank Paul Haines for reading the manuscript. Numerical Computation of this work was carried out at the Yukawa Institute Computer Facility. N. Sakai was supported by JSPS

Research Fellowships for Young Scientists. This work was supported partially by the Grant-in-Aid for Scientific Research Fund of the Ministry of Education, Science and Culture (No.9702603, No.09740334, and No.09440106).

A. On Double Lorentz Transformation

In this Appendix we show the equations of the double ‘‘Lorentz transformation’’ (5) can be derived exactly from a general coordinate transformation in a curved spacetime. Here we demonstrate the transformation at $t = t_1$ and omit the subscript 1.

First, we have to introduce another coordinate system which overlaps both the Einstein-de Sitter background and the Minkowski region. We adopt a Gaussian normal coordinate system $(\tau, n, \theta, \varphi)$ in which $n = 0$ represents the world-hypersurface of the shell. τ is chosen to be the proper time of the shell. i.e., the 3-metric at $n = 0$ is give by

$$ds^2 = -d\tau^2 + R^2(\tau)(d\theta^2 + \sin^2 \theta d\varphi^2). \quad (\text{A1})$$

The coordinate transformation of the 4-momentum k_{EdS}^μ at $n = 0$ from the Einstein-de Sitter frame $\{x_{\text{EdS}}^\mu\}$ to the Gaussian normal frame $\{y_{\text{GN}}^\nu\}$ is given by

$$k_{\mu}^{\text{GN}} = \frac{\partial x_{\text{EdS}}^\nu}{\partial y_{\text{GN}}^\mu} k_{\nu}^{\text{EdS}}. \quad (\text{A2})$$

It is easy to find

$$\frac{\partial t}{\partial \tau} = \gamma, \quad \frac{\partial r}{\partial \tau} = \frac{\gamma v}{a}, \quad (\text{A3})$$

and Sakai & Maeda (1993) obtained

$$\frac{\partial t}{\partial n} = \gamma v, \quad \frac{\partial r}{\partial n} = \frac{\gamma}{a}. \quad (\text{A4})$$

If we write the 4-momentum in each frame as

$$k_{\text{EdS}}^\mu = E \left(1, \frac{\cos \psi}{a}, \frac{\sin \psi}{ar}, 0 \right), \quad k_{\text{GN}}^\mu = E'' \left(1, \cos \psi'', \frac{\sin \psi''}{R}, 0 \right), \quad (\text{A5})$$

equation (A2) reduces

$$E'' = E\gamma(1 + v \cos \psi), \quad E'' \cos \psi'' = E\gamma(v + \cos \psi). \quad (\text{A6})$$

This is nothing but the expression of a usual Lorentz transformation. If we also carry out the coordinate transformation of the 4-momentum from the Gaussian normal frame to the Minkowski frame in the similar way, the expression of the double Lorentz transformation (5) is obtained.

B. Derivation of Thin Lens Equation

Here we derive the lens equation (22) from null geodesic equations. As depicted in Figure 1, we introduce a vector basis, $\{\mathbf{n}(\alpha), \mathbf{l}(\alpha)\}$, in the two-dimensional comoving space, and denote each position by a vector symbol \mathbf{r} . The trajectory of a photon in a homogeneous region is

$$\mathbf{r}_2 - \mathbf{r}_0 = \int_{t_2}^{t_0} \frac{dt}{a} \mathbf{n} = 3t_0(1 - \sqrt{a_2})\mathbf{n}, \quad (\text{B1})$$

$$\mathbf{r}_{\text{LSS}} - \mathbf{r}_1 = \int_{t_1}^{t_{\text{LSS}}} \frac{dt}{a} (\cos \delta \alpha \mathbf{n} + \sin \delta \alpha \mathbf{l}) = 3t_0 \left[(\sqrt{a_1} - \sqrt{a_{\text{LSS}}}) (\mathbf{n} + \delta \alpha \mathbf{l}) + O(\zeta^3) \right], \quad (\text{B2})$$

where we have expanded the equations with a dimensionless parameter,

$$\zeta \equiv \frac{r_2}{3t_0}. \quad (\text{B3})$$

To get the last equality of (B2), we have used the facts that $\delta \alpha$ is of order $(H_2 R_2)^2$ and that $H_2 R_2$ is of order ζ . Explicitly, the geodesic between \mathbf{r}_0 and \mathbf{r}_2 says equation (20) and

$$H_2 R_2 = \frac{2\zeta}{1 - d \cos \alpha / 3t_0 + \zeta \cos \psi_2}, \quad (\text{B4})$$

and hence equation (8) is rewritten as

$$\delta \alpha = \frac{8q\sqrt{1-q^2}}{(1 - d \cos \alpha / 3t_0)^2} \zeta^2 + O(\zeta^3) \quad \text{with} \quad q \equiv \frac{d}{r_2} \sin \alpha. \quad (\text{B5})$$

As for $\mathbf{r}_1 - \mathbf{r}_2$, we obtain

$$\mathbf{r}_1 - \mathbf{r}_2 = [r_1 \cos(\delta + \psi_1) + r_2 \cos \psi_2] \mathbf{n} + [r_1 \sin(\delta + \psi_1) - r_2 \sin \psi_2] \mathbf{l}. \quad (\text{B6})$$

In order to expand $\delta + \psi_1$, r_1 and $\sqrt{a_1}$ with ζ (or $H_2 R_2$), we use the relations

$$H_1 R_1 = H_2 R_2 - (3\beta - 1) \cos \psi_2 (H_2 R_2)^2 + \frac{3}{2} (3\beta - 1) \left[\left(\beta - \frac{2}{3} \right) \cos^2 \psi_2 + \beta \right] (H_2 R_2)^3 + O\left((H_2 R_2)^4\right), \quad (\text{B7})$$

$$\psi_1 = \psi_2 + 3\beta H_2 R_2 \sin \psi_2 + O\left((H_2 R_2)^2\right), \quad (\text{B8})$$

which are found in the derivation of TV's formula (7) and (8). Then we obtain

$$\mathbf{r}_1 - \mathbf{r}_2 = r_2 (2 \cos \psi_2 - 3\beta H_2 R_2) \mathbf{n} + 3t_0 O(\zeta^3) = 3t_0 [(\sqrt{a_2} - \sqrt{a_1}) \mathbf{n} + O(\zeta^3)]. \quad (\text{B9})$$

Equation (B9) tells us that, although a photon is bent inside the void, the deviation is of order ζ^3 . From equations (B1)-(B4), (B9), and the relation,

$$\sqrt{a_1} = \sqrt{a_2} + O(\zeta) = 1 - \frac{d \cos \alpha}{3t_0} + O(\zeta), \quad (\text{B10})$$

we find

$$\begin{aligned} \mathbf{r}_{\text{LSS}} - \mathbf{r}_0 &= 3t_0 \left[(1 - \sqrt{a_{\text{LSS}}}) \mathbf{n} + \left(1 - \frac{d \cos \alpha}{3t_0} - \sqrt{a_{\text{LSS}}} \right) \delta \alpha \mathbf{l} + O(\zeta^3) \right] \\ &= (\mathbf{r}_{\text{LSS}} - \mathbf{r}_0)_b + (d_{\text{LSS}} - d \cos \alpha) \delta \alpha \mathbf{l} + 3t_0 O(\zeta^3), \end{aligned} \quad (\text{B11})$$

where the subscript b denotes a background unperturbed quantity. We thus reach equation (22), i.e.,

$$\delta \boldsymbol{\theta} \equiv \frac{\mathbf{r}_{\text{LSS}} - \mathbf{r}_{\text{LSS},b}}{d_{\text{LSS}}} = \frac{d_{\text{LSS}} - d \cos \alpha}{d_{\text{LSS}}} \delta \alpha \mathbf{l} + O(\zeta^3). \quad (\text{B12})$$

This result provides us a simple description: as long as we look at the leading terms of ζ , a void can be regarded to be a “thin lens” with a scattering angle $\delta \alpha$.

REFERENCES

- Amendola, L., Baccigalupi, C., Konoplick, R., Occhionero, F., & Rubin, S. 1996, *Phys. Rev. D*, 54, 7199
- Arnau, J.V., Fullana, M.J., Monreal, L., & Saez, D. 1993, *ApJ*, 402, 359
- Baccigalupi, C. 1997, *ApJ*, in press
- Baccigalupi, C., Amendola, L., Fortini, P., & Occhionero, F. 1997, *Phys. Rev. D*, 56, 4610
- Baccigalupi, C., Amendola, L., & Occhionero, F. 1997, *MNRAS*, 288, 387
- Bertschinger, E. 1985, *ApJS*, 58, 1
- Blanchard, A., & Schneider, J. 1987, *A&A*, 184, 1
- Cayón, C., Martínez-González, E., & Sanz, J.L. 1993a, *ApJ*, 403, 471
- Cayón, C., Martínez-González, E., & Sanz, J.L. 1993b, *ApJ*, 413, 10
- Cole, S., & Efstathiou, G. 1989, *MNRAS*, 239, 195
- da Costa, L.N. et al. 1994, *ApJ*, 424, L1
- El-Ad, H., & Piran, T. 1997, *astro-ph/9702135*.
- El-Ad, H., Piran, T., & da Costa, L.N. 1996, *ApJ*, 462, L13
- El-Ad, H., Piran, T., & da Costa, L.N. 1997, *MNRAS*, 287, 790
- Fukushige, T., Makino, J., & Ebisuzaki, T. 1994, *ApJ*, 436, L107
- Fullana, M.J., Arnau, J.V., & Saez, D. 1996, *MNRAS*, 280, 1180

- Geller M.J., & Huchra J.P. 1989, *Science*, 246, 897
- Hu, W., Sugiyama, N., & Silk, J. 1997, *Nature*, 386, 37
- Kashlinsky, A. 1988, *ApJ*, 331, L1
- La, D. 1991, *Phys. Lett. B*, 265, 232
- Liddle, A.R., & Wands, D. 1991, *MNRAS*, 253, 637
- Linder, V.E. 1990a, *MNRAS*, 243, 353
- Linder, V.E. 1990b, *MNRAS*, 243, 362
- Maeda, K., & Sato, H. 1983, *Prog. Theor. Phys.*, 70, 772
- Martínez-González, E., & Sanz, J.L. 1990, *MNRAS*, 247, 473
- Martínez-González, E., Sanz, J.L., & Cayón, C. 1997, *ApJ*, 484, 1
- Martínez-González, E., Sanz, J.L., & Silk, J. 1990, *ApJ*, 355, L5
- Mészáros, A. 1994, *ApJ*, 423, 19
- Mészáros, A., & Molnár, Z. 1996, *ApJ*, 468,
- Occhionero, F., & Amendola, L. 1994, *Phys. Rev. D*, 50, 4846
- Panek, M. 1992, *ApJ*, 388, 225
- Rees, M.J., & Sciama, D.W. 1968, *Nature*, 217, 511
- Sachs, R.K., & Wolfe, A.M. 1967, *ApJ*, 147, 73
- Sakai, N., & Maeda, K. 1993, *Prog. Theor. Phys.*, 90, 1001
- Sasaki, M. 1989, *MNRAS*, 240, 415
- Sato, H. 1985, *Prog. Theor. Phys.*, 73, 649
- Seljak, U. 1996, *ApJ*, 463, 1
- Shi, X., Widrow, L.M., & Dursi, L.J. 1996, *MNRAS*, 281, 565
- Thompson, K.L., & Vishniac, E.T. 1987, *ApJ*, 313, 517
- Tomita, K. 1989, *Phys. Rev. D*, 40, 3821
- Tomita, K., & Watanabe, K. 1989, *Prog. Theor. Phys.*, 82, 563
- Turner, M.S., Weinberg, E.J., & Widrow, L.M. 1992, *Phys. Rev. D*, 46, 2384

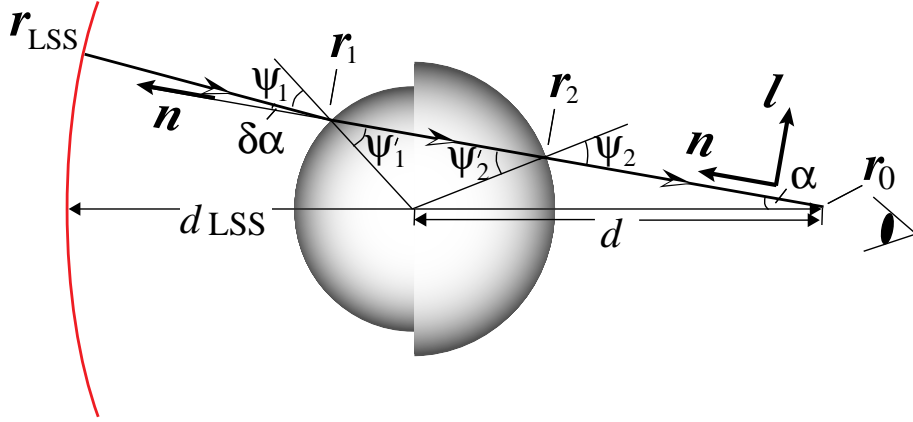


Fig. 1.— Cross section of a void on the $\varphi = \pi/2$ plane (TV’s model). We depict the trajectory of a photon from the LSS to an observer. The subscripts 1 and 2 denote quantities at the time the photon enters the void and at the time it leaves, respectively. The subscripts LSS and 0 denote quantities at the LSS and at present, respectively. Define α as the angle formed between the direction of observation and the direction of the void’s center, $\delta\alpha$ as the scattering angle of a photon, d as the comoving distance of the void’s center, and d_{LSS} as the comoving distance of the LSS. For Appendix B we denote each position by a vector symbol \mathbf{r} , and introduce a vector basis, $\{\mathbf{n}(\alpha), \mathbf{l}(\alpha)\}$, in the two-dimensional comoving space.

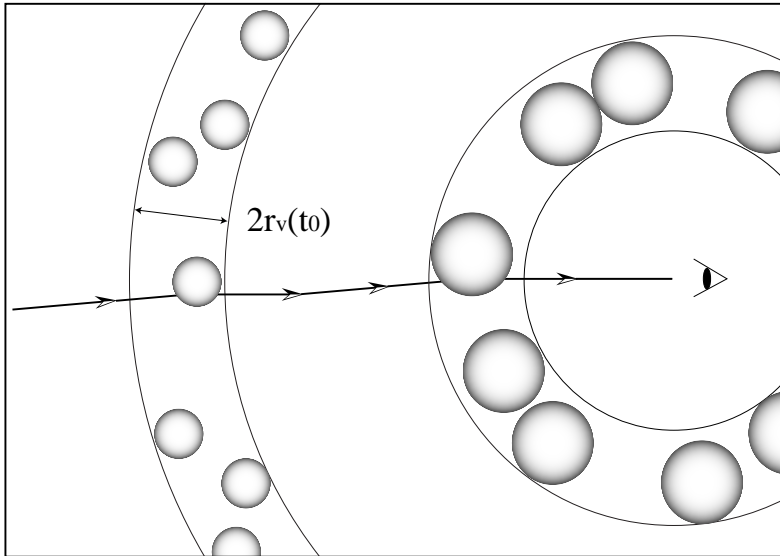


Fig. 2.— Schematic sketch of a void-network universe (TV’s model). Divide the universe into shells of comoving thickness $2r_v(t_0)$.

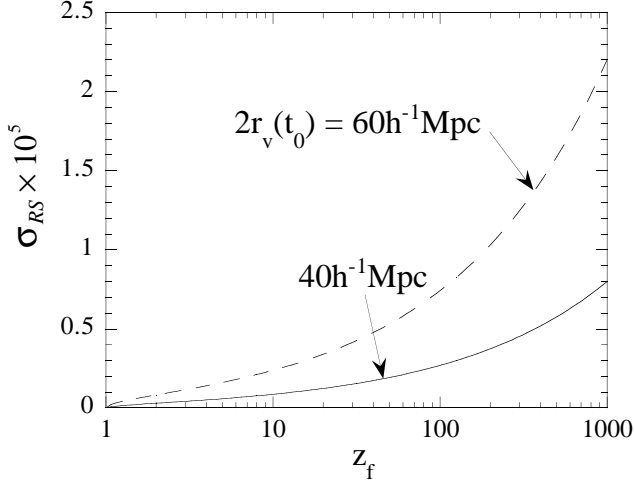


Fig. 3.— RS effect: plot of eq. (14) (TV’s results) for $2r_v(t_0) = 40h^{-1}\text{Mpc}$ and $60h^{-1}\text{Mpc}$. We set $\beta = 0.13$ and $F_0 = 2/3$.

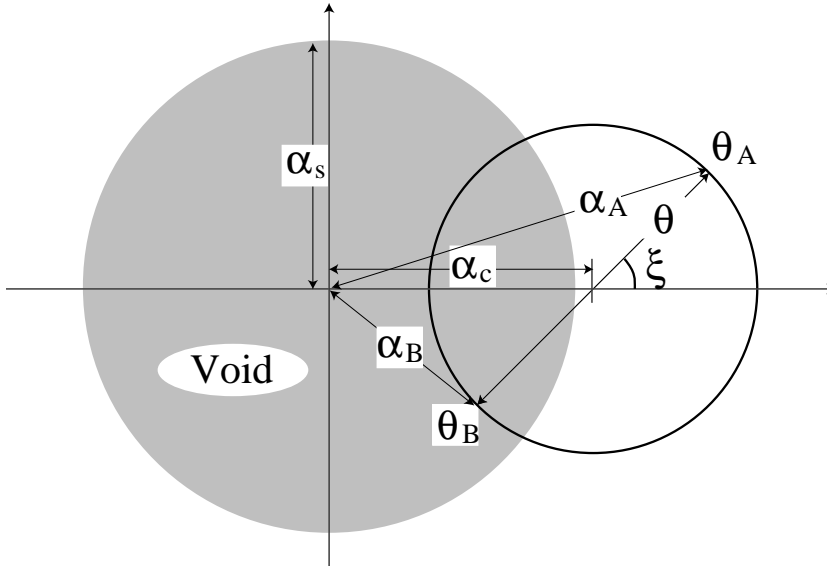
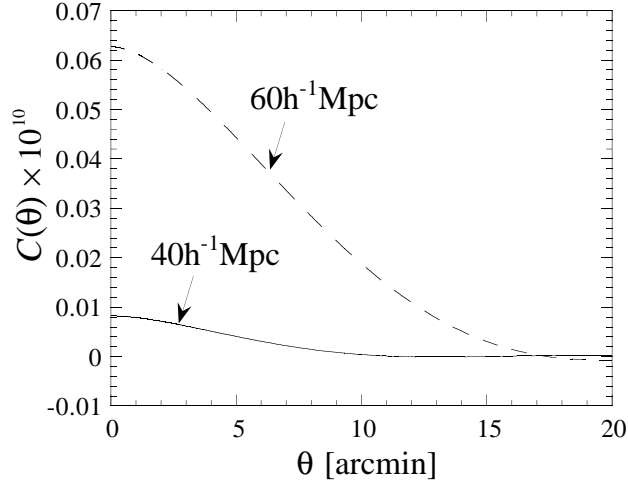
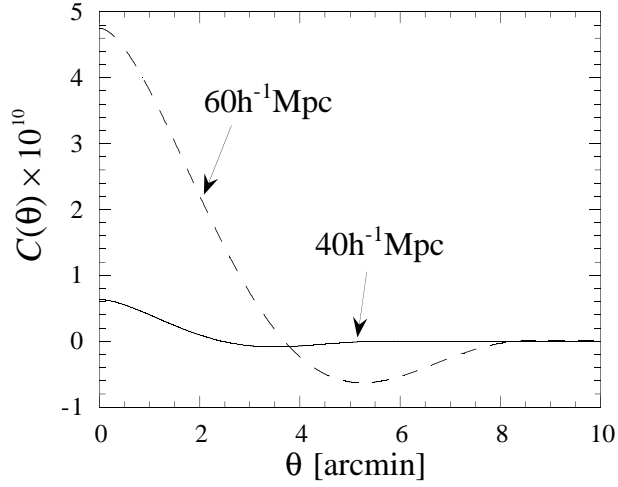


Fig. 4.— Projection of a void on the celestial sphere. Neglecting the curvature of the sphere in a local region around a void, we consider two light rays, which are labeled as θ_A and θ_B .



(a)



(b)

Fig. 5.— RS effect: plots of $C(\theta)$ v.s. θ for (a) $z_f = 5$ and for (b) $z_f = 1000$. We set $\beta = 0.13$ and $F_0 = 2/3$.

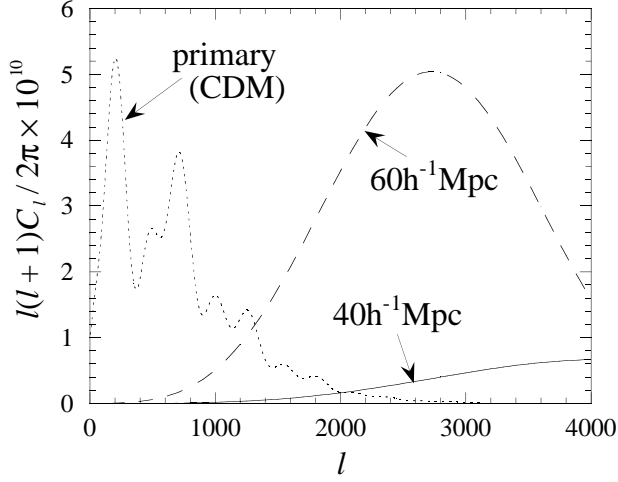


Fig. 6.— RS effect: plot of the CMB angular power spectrum $l(l+1)C_l$ v.s. l for $C(\theta)$ in Fig. 5(b). For reference, we also plot the values of C_l estimated for a CDM model.

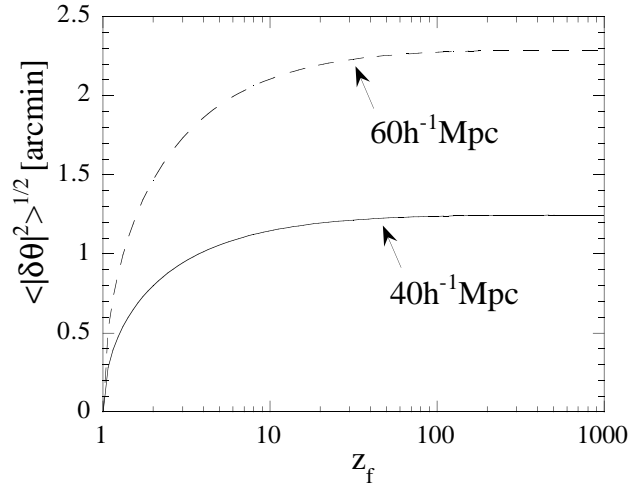


Fig. 7.— Lensing effect: plot of $\sqrt{\langle |\delta\theta|^2 \rangle}$ v.s. z_f . We set $\beta = 0.13$, $F_0 = 2/3$, and $z_{\text{LSS}} = 1000$.

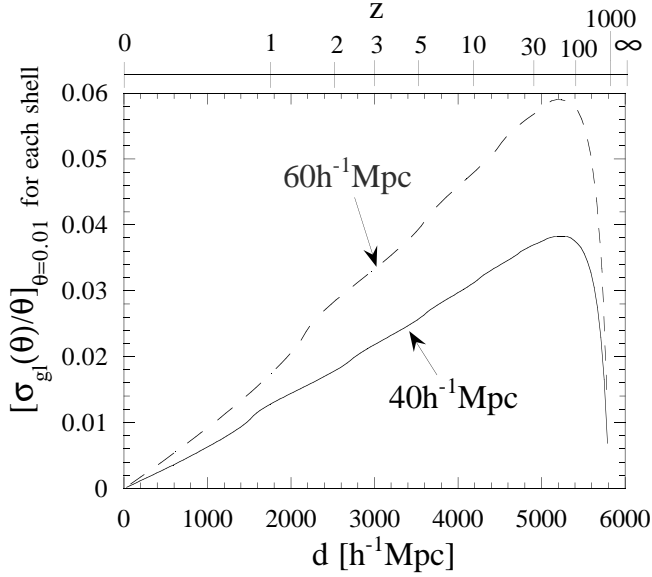


Fig. 8.— Lensing effect: plot of $[\sigma_{gl}(\theta)/\theta]_{\theta=0.01\text{arcmin}}$ for each shell v.s. the position of shells ($h^{-1}\text{Mpc}$ and z). We set $\beta = 0.13$, $F_0 = 2/3$, and $z_{\text{LSS}} = 1000$.

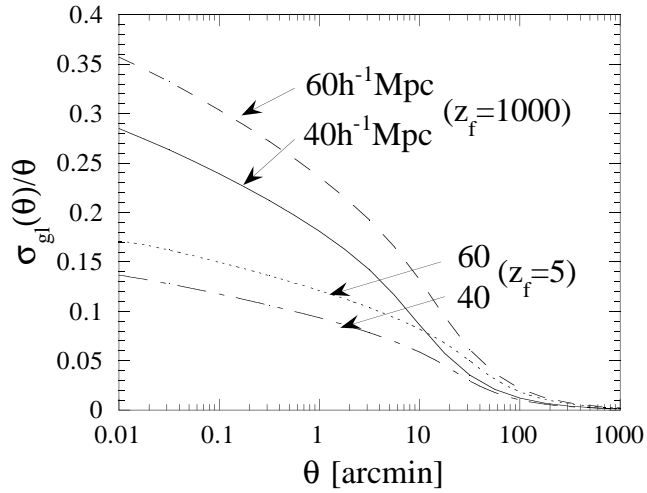
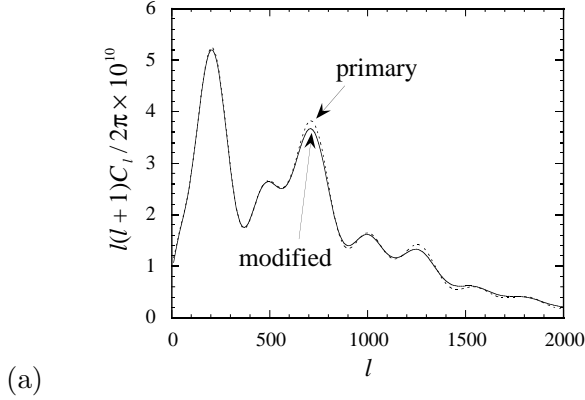
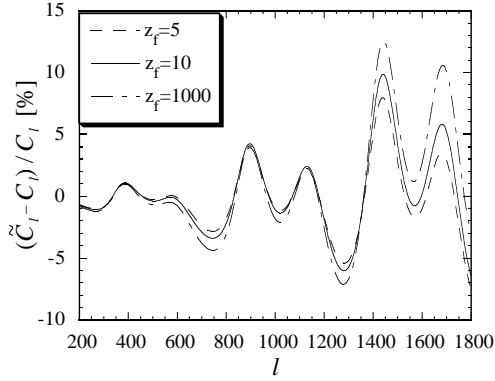


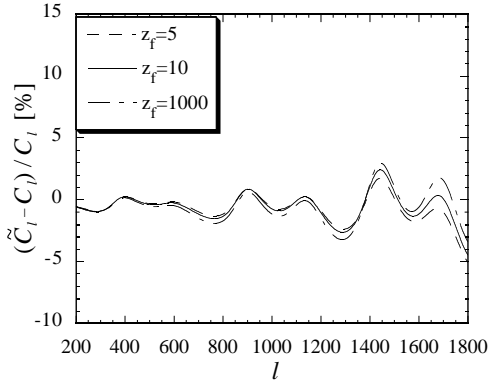
Fig. 9.— Lensing effect: plot of $\sigma_{gl}(\theta)/\theta$ v.s. θ . We set $\beta = 0.13$, $F_0 = 2/3$, and $z_{\text{LSS}} = 1000$



(a)



(b)



(c)

Fig. 10.— Lensing effect. (a) shows plots of the CMB angular power spectrum $l(l+1)C_l$ v.s. l with lensing and without lensing for $2R_0 = 60h^{-1}\text{Mpc}$ and $z_f = 1000$. In (b) and in (c), respectively, the relative changes of the spectrum due to lensing for $2R_0 = 60h^{-1}\text{Mpc}$ and for $2R_0 = 40h^{-1}\text{Mpc}$ are presented. We set $\beta = 0.13$, $F_0 = 2/3$, and $z_{\text{LSS}} = 1000$.